# Synthesis, Molecular Docking Study and Cytotoxicity Evaluation of some Quinazolinone Derivatives as Nonclassical Antifolates and Potential Cytotoxic Agents

## Mohammed Abdulameer Oleiwi [*,1] and Munaf H. Zalzala [**]

[*]Department of Pharmaceutical Chemistry, College of Pharmacy, University of Baghdad, Baghdad, Iraq.
[**]Department of Pharmacology and Toxicology, College of Pharmacy, University of Baghdad, Baghdad, Iraq.

## Abstract

New 4(3H)-quinazolinone derivatives (S1-S4) were synthesized and characterized by FTIR, ^{1}HNMR, and ^{13}CNMR. Their cytotoxic activity against a set of human cancer cell lines MCF-7 (breast) and A549 (lung) was evaluated using MTT assay. To detect their selectivity toward cancer cells, the compounds were also tested against epithelial cells derived from normal human fibroblast (NHF). Methotrexate (MTX) was used as a positive control. All the tested compounds (S1-S4) exhibited toxicity against the normal cells lower than cancer cells. With the exception of compounds (S3 and S4), the tested compounds showed no siginificant differences from MTX regarding their inhibition rate against the normal cells (NHF) in all concentrations. All tested compounds displayed higher cytotoxicity against the lung cancer cell line (A549) than MTX with the most potent one is being compound S2 ($IC_{50}$: 5.73 µM). Among the tested compounds, compound S1 exhibited the highest cytotoxic activity against the breast cancer cell line (MCF-7) ($IC_{50}$: 3.38 µM) compared to MTX ($IC_{50}$: 27.32 µM). The binding modes of the synthesized compounds with the target proteins (DHFR and TS) were investigated by molecular docking studies using GOLD software. Molecular docking study showed that both compounds S1 and S2 displayed partially a similar binding mode with the active site of DHFR in comparison with the co-crystallized ligand (MTX), whereas compound S1 showed a different binding mode with the active site of TS when compared with the co-crystallized ligand (raltitrexed).

**Keywords: 4(3H)-quinazolinone, DHFR, 1,3,4-Thiadiazole, Thymidylate synthase.**

## تصنيع ودراسة التراصف الجزيئي وتقييم السمية الخلوية لبعض مشتقات الكينازولينون كمضادات غيرتقليدية للفولات و عوامل ذات سمية خلوية محتملة

### محمد عبد الأمير عليوي *¹ و مناف هاشم زلزلة **

*فرع الكيمياء الصيدلانية ، كلية الصيدلة ، جامعة بغداد، بغداد، العراق.
** فرع الادوية والسموم ، كلية الصيدلة ، جامعة بغداد، بغداد ،العراق.

### الخلاصة

تم تصنيع سلسلة من مشتقات ال ٤ (3H) - كينازولينون الجديدة (S1-S4) وتم تشخيصها بواسطة طيف الاشعة تحت الحمراء والرنين النووي المغناطيسي كما تم تقييم فعاليتها السمية ضد مجموعة من الخلايا السرطانية البشرية وهي MCF-7 (الثدي) و A549 (الرئة) باستخدام مقايسة MTT ، تم اختبار المركبات أيضًا ضد الخلايا الظهارية المشتقة من الخلايا الليفية البشرية الطبيعية (NHF) للكشف عن مدى انتقائيتها تجاه الخلايا السرطانية .تم استخدام عقار الميثوتريكسيت كعنصرتحكم ايجابي. أظهرت جميع المركبات المختبرة سمية ضد الخلايا الطبيعية بدرجة أقل من خطوط الخلايا السرطانية المختارة كما أظهرت جميع المركبات سمية خلوية أعلى ضد خط خلايا سرطان الرئة (A549) من الميثوتريكسيت وكان المركب S2 هوالاعلى فاعلية ($IC_{50}$:5.73µM) . من بين المركبات التي تم اختبارها ضد خط خلايا سرطان الثدي (MCF-7)اظهر المركب S1 الفاعلية الاعلى ( $IC_{50}$:3.38 µM ) بالمقارنة مع الميثوتريكسيت ($IC_{50}$: 27.32 µM) كما تم فحص أوضـاع الارتباط للمركبات المصنعة مع البروتينات المستهدفة (DHFR) و (TS) من خلال دراسات التراصف الجزيئي باستخدام برنامج GOLD . أظهرت دراسة التراصف الجزيئي أن كلا المركبين S1 و S2 اظهرا جزئيا وضـع ربط مماثل مع الموقع النشـط ل DHFR بالمقارنة مع ليغاند المتبلور المشـترك (MTX), بينماً أظهر المركب S1 وضـع ربط مختلف مع الموقع النشـط ل TS بالمقارنة مع ليغاند المتبلور المشـترك (raltitrexed).

الكلمات المفتاحية: كينازولينون -4(3H), مختزل ثنائي هيدروفولات, ثياديازول-1,3,4 , ثيميدلات سينثيز.

## Introduction

The major problems associated with the current chemotherapeutic drugs are represented by multidrug-resistant tumours and severe systemic toxicity [1]. Compounds that are designed to hit a single biological target often have limited clinical benefit in the treatment of complex diseases such as cancer, therefore the strategy of designing a single drug with multiple targets is considered as an alternative therapeutic approach [2].

*Iraqi Journal of Pharmaceutical Science*

The dependence of rapidly dividing cells on the availability of nucleotide precursors provides an attractive therapeutic target for the development of new anticancer agents, the most widely utilized among these targets is the folate biosynthesis pathway that leads to thymidine synthesis [3]. Dihydrofolate reductase (DHFR) and thymidylate synthase (TS) are the key enzymes in folate metabolism which is necessary for the synthesis of DNA, RNA, and proteins [4]. Antifolates are structurally related to folate derivatives, their antitumor activity is attributed to their ability to inhibit the folate-dependent enzymes [5]. Antifolates are divided into two classes; classical antifolates that possesses a glutamate tail and must be actively transported into the cell utilizing a carrier known as Reduced folate carrier (RFC), and non-classical antifolates, these are lipophilic inhibitors that cross the cell membrane by passive diffusion [3].The cytotoxic activity of classical antifolates is highly dependent upon the glutamate component, which is necessary for the active uptake into cells via the reduced folate carrier. This component is further polyglutamated by an enzyme called folylpolyglutamate synthetase (FPGS) [6]. Cancer cells develop resistance to classical antifolates such as raltitrexed, which depend on polyglutamylation for their antitumor activity by producing defective folylpoly-γ-glutamate synthetase (FPGS) enzyme or reducing its synthesis [7]. Therefore, to overcome these potential disadvantages associated with classical antifolates, nonclassical antifolates have been designed and synthesized [8]. These lipophilic nonclassical antifolates lack the polar glutamate moiety and, therefore, do not require FPGS for their antitumor activity (Figure 1) [9].
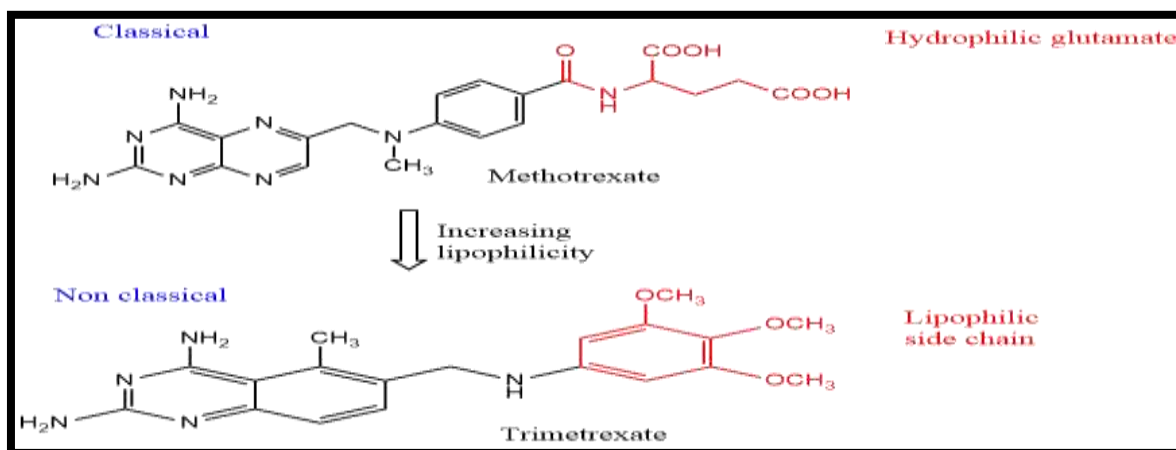


**Figure 1. Classification of antifolate drugs.**

4(3H)-quinazolinone scaffold has drawn much attention in the field of drug design and developments due to its wide spectrum of biological activities, mainly its cytotoxic potential [10].The anticancer activity of quinazolinone derivatives depend on their ability to inhibit many enzymes essential in cell division such as thymidylate synthase (TS) [11, 12] and dihydrofolate reductase (DHFR) enzymes [13]. On the other hand, 1,3,4-thiadiazole scaffold was found to possess a promising antitumor activity against many cancer cell lines through the inhibition of many molecular targets, such as tyrosine kinase and histone deacetylase (HDAC) [14]. The aim of this research was to synthesize some quinazolinone derivatives as nonclassical antifolates and possible inhibitors of dihydrofolate reductase and thymidylate synthase enzymes.

## Materials and Methods

All reagents, chemicals, and solvents used in the chemical synthesis were used as obtained from their suppliers. 6-(bromomethyl)-2-methyl-4(3H)-quina- zolinone was purchased from Henan Tianfu Chemical Co. (China). 5-methylamino-1,3,4-thiadiazole-2-thiol was purchased from Apollo Scientific (UK), methotrexate was purchased from (Mylan) company (France).The progress of the reactions and purity of the products were checked by thin layer chromatography (TLC) on pre-coated aluminium sheets Silica Gel 60 F254 (Merck) and the spots were visualized under a 254 nm UV lamp. Melting points were determined by open capillary method using the Stuart SMP3 apparatus (UK). Fourier Transform Infrared (FTIR) Spectroscopy was done utilizing Shimadzu IRAffinity-1 Spectrometer (Japan) and Specac® ATR- diamond type (UK). ¹HNMR and ¹³CNMR analysis were performed using the Bruker and Varian model ultrashield spectrometer at 500 MHz for ¹HNMR and 125 MHz for ¹³CNMR with tetramethylsilane (TMS) as the internal standard and *d6*-DMSO or CDCl₃ as the solvent. Chemical shift values are expressed in the δ (ppm) scale and the signals are described as s (singlet), d (doublet), m (multiplet), and b (broad) whereas coupling constants (J) are expressed in hertz. Cytotoxicity assay was performed at the Iraqi Biotech. Research Centre (Baghdad, Iraq) using fetal bovine serum (FBS), Trypsin/EDTA and Roswell Park Memorial Institute

(RPMI)1640 medium (Capricorn, Germany), Cell culture plates and dimethylsulfoxide (DMSO) (Santacruz Biotechnology, USA), (MTT) stain (Bio-World, USA) ), microtiter reader (Gennex lab., India ), laminar flow hood and $CO_2$ incubator (Cypress Diagnostics, Belgium). The crystallized structures of DHFR (PDB: 3EIG) [15] and TS (PDB: 5X5Q) [16] were downloaded from the protein data bank (PDB, www.rcsb.org) [17].

### General synthesis of compounds (A1-A4)

The synthesis of compounds (A1-A4) was done according to the following procedure [18].
To a stirred solution of aniline or substituted anilines (20 mmol) in 25 ml of dry benzene, TEA (20 mmol) was added, the mixture was stirred on the ice bath, then chloroacetylchloride (24 mmol) (dissolved in 20 ml of dry benzene) was added drop wise in 30 min. The mixture was then refluxed for 3 h. The excess of solvent (benzene) was evaporated under vacuum and the precipitate was washed with sodium carbonate (2%), HCl (5%), and distilled water, then dried and recrystallized from ethanol.

### 2-chloro-N-Phenylacetamide (A1)

Light yellow powder, yield 78%, m.p (131-133$^0$C). Rf =0.74 (n-hexane: ethyl acetate: methanol 5:3:2). FTIR (υ, cm$^{-1}$), 3267(NH) str. of sec. amide, 3097 Ar (C-H), 1666 (C=O) str. of amide ,748 (C-Cl) str. $^1$HNMR (DMSO-*d6*, 500 MHz, δ=ppm):4.23(s,2H,CH$_2$-Cl),7.07(t,1H, Ar-H),7.31(m,2H,Ar-H), 7.57 (d, 2H ,J= 8.47, Ar-H),10.27(bs,1H, NH).$^{13}$CNMR (DMSO-*d6*, 125MHz): 44.03, 119.79 ,124.27,129.29,138.91,165.04.

### 2-chloro-N-(4-chlorophenyl) acetamide (A2).

White crystals, yield 86%, m.p (172-174$^0$C), Rf =0.83 (n-hexane: ethyl acetate: methanol 5:3:2). FTIR (υ, cm$^{-1}$),3263(NH) str. of sec. amide, 3086 Ar(C-H),1666 (C=O) str. of amide, 775 (C-Cl) str. $^1$HNMR(DMSO-*d6*, 500MHz ,δ= ppm) :4.24(s,2H,CH$_2$-Cl),7.37(d, 2H, J= 8.50Hz, Ar-H), 7.60 (d, 2H, J=8.50Hz, Ar-H) ,10.39(bs,1H,NH).$^{13}$CNMR (DMSO-*d6*,125MHz):43.95, 121.35, 127.88, 129.21 , 137.86,165.22.

### 2-chloro-N-(4-methoxyphenyl) acetamide (A3).

Gray powder, yield 94%, m.p (116-118$^0$C), Rf =0.81(n-hexane: ethyl acetate: metanol 5:3:2). FTIR (υ, cm$^{-1}$),3294(NH) str. of sec. amide, 3074 Ar(C-H ),1662 (C=O) str. of amide, 1246 (C-O) str., 786 (C-Cl) str. $^1$HNMR (DMSO-*d6*, 500MHz, δ=ppm): 3.71(s,3H,O-CH$_3$), 4.19 (s, 2H,CH$_2$-Cl), 6.89 (d,2H ,J=8.37Hz ,Ar-H),7.48(d, 2H,J=8.37Hz, Ar-H), 10.11 (bs,1H,NH). $^{13}$CNMR (DMSO-*d6*, 125MHz): 48.72, 60.41, 119 .17, 126.18, 136.76, 160.84, 169.32.

### 2-chloro-N-(4-nitrophenyl) acetamide (A4).

Green powder, yield 88%, m.p (179-181$^0$C), Rf =0.78 (n-hexane: ethyl acetate: methanol 5:3:2). FTIR (υ, cm$^{-1}$), 3275(NH) str. of sec. amide, 3070Ar(C-H) ,1685(C=O) str. of amide ,1566,1334 asymmetric and symmetric str. of (NO$_2$), 748 (C-Cl) str. $^1$HNMR (DMSO-*d6*, 500MHz, δ=ppm): 4.32 (s,2H,CH$_2$-Cl),7.82 (d,2H, J=7.28, Ar-H),8.23(d, 2H, J=7.28, Ar-H),10.82(bs,1H,NH).$^{13}$CNMR (DMSO-*d6*,125MHz): 44.01,119.48,125.38,143.02,145.00 ,165.98 .

### General synthesis of compounds (B1-B4).

The synthesis of compounds (B1-B4) was done according to the following procedure [19].
To a stirred suspension of 5-methylamino-1,3,4-thiadiazole-2-thiol (1.7 mmol) in 10 ml distilled water, TEA (2 mmol) was added and the mixture was stirred until the compound completely dissolve, then one of the compounds (A1-A4) (1.7 mmole) was dissolved in (3 ml) of DMF and added gradually to the aqueous solution with stirring which was continued for 3 h. (Monitored with TLC). The product was collected by filtration, washed with distilled water (3x50ml), dried, and recrystallized from ethanol.

### 2-((5-(methylamino)-1,3,4-thiadiazol-2-yl)thio)-N-phenylacetamide (B1).

Light brown powder, yield 68%, m.p (147-149$^0$C), Rf =0.61(n-hexane: ethyl acetate: methanol 5:3:2). FTIR (υ,cm$^{-1}$),3290 (NH) str .of sec. amine ,3267 (NH) str.of sec. amide, 3086 Ar (C-H) ,1685 (C=O) str. of amide ,1600 (C=N) str. $^1$HNMR (DMSO-*d6*, 500MHz, δ=ppm) :2.86(s,3H,NH-CH$_3$),3.98(s,2H,CH$_2$-S-) ,7.05(t,1H,Ar-H),7.30(m,2H,Ar-H), 7.56(d,2H,J=8.06,Ar-H), 7.70 (bs, 1H, NH, sec.amine),10.20(bs,1H,NH,sec. amide).$^{13}$CNMR(DMSO-*d6*, 125MHz): 31.52, 39.34, 119.63, 124.01, 129.24, 139.21, 149.35, 166.19, 171.12.

### N-(4-chlorophenyl)-2-((5-(methylamino)-1,3,4-thiadiazol-2-yl) thio)acetamide (B2).

Light yellow powder, yield 77%, m.p (203-205$^0$C), Rf =0.58 (n-hexane: ethyl acetate: methanol 5:3:2). FTIR (υ,cm$^{-1}$),3282 (NH) str. of sec. amine, 3255(NH) str.of sec. amide, 3059 Ar(C-H),1685(C=O) str. of amide, 1608 (C=N) str. $^1$HNMR(DMSO-*d6*, 500MHz, δ=ppm):2.88(s,3H, NH-CH$_3$),4.01(s,2H, CH$_2$-S-), 7.36 (d,2H, J=8.60Hz, Ar-H),7.58(d,2H, J=8.60 Hz, Ar-H),7.84(bs ,1H,NH ,sec. amine) ,10.34 (bs ,1H, NH, sec. amide) .$^{13}$CNMR (CDCl$_3$, 125MHz):36.29, 44.03, 125.93 ,132.35 ,133.93 ,142.93 ,153.97,171.16,175.88.

### N-(4-methoxyphenyl)-2-((5-(methylamino)-1,3,4-thiadiazol-2-yl)thio)acetamide (B3).

Off-white powder, yield 76%, m.p (151-153$^0$C), Rf =0.56 (n-hexane: ethyl acetate: methanol 5:3:2). FTIR(υ, cm$^{-1}$),3363(NH)str. of sec. amine, 3217 (NH) str .of sec. amide, 3001 Ar (C-H), 1654 (C=O) str. of amide ,1608 (C=N) str., 1234(C-O) str.$^1$HNMR (DMSO-*d6*, 500MHz, δ=ppm) :2.83 (s,3H ,NH-CH$_3$)3.70(s, 3H ,O-CH$_3$),3.93(s,2H, CH$_2$-S-),6.87(d, 2H , J= 8.55 Hz, Ar-H) ,7.45 (d,2H,

J =8.55 Hz , Ar-H),7.69 (bs,1H, NH, sec. amine ),10.06 (bs, 1H, NH, sec. amide) . ^{13}CNMR (DMSO-*d6*, 125MHz): 31.51, 39.24, 55.61, 114.37, 121.15, 132.35, 149.97, 155.86, 165.65, 171.09.

***2-((5-(methylamino)-1,3,4-thiadiazol-2-yl)thio)-N-(4-nitrophenyl)acetamide (B4).***

Beige powder, yield 73%, m.p (219-221[0]C), Rf =0.53 (n-hexane: ethyl acetate: methanol 5:3:2). FTIR (υ, cm[−1]),3332 (NH) str. of sec. amine, 3282 (NH) str. of sec. amide, 3089 Ar (C-H) str.,1697 (C=O) str .of amide, 1616 (C=N) str. ,1554,1330 asymmetric and symmetric str. of (NO₂).^{1}HNMR(DMSO-*d6*, 500MHz, δ=ppm): 2.85(s,3H, NH-C$\underline{H}$₃), 4.04 (s,2H, C$\underline{H}$₂-S-), 7.70 (bs, 1H, NH, sec. amine),7.80(d,2H, J=9.14Hz, Ar-H), 8.22 (d,2H, J=9.14Hz , Ar-H),10.82 (bs, 1H,NH,sec.amide).^{13}CNMR(DMSO-*d6*,125MHz): 31.52 ,39.27 ,119.32 ,125.51 ,142.86,145.31 ,148.87,167.33,172.45.

***General synthesis of compounds (S1-S4)***

The synthesis of the target compounds (S1-S4) was done according to the following procedure [(20,21)].

A solution of 6-(bromomethyl)-2-methyl-4(3H)-quinazolinone (1.48 mmol) in dry DMF (10 ml) was added gradually to a mixture of one of the compounds (B1-B4) (1.48 mmol) and dry TEA (1.48 mmol) in dry DMF (15 ml) and the reaction mixture has been stirred at 80 [0]C overnight. The solvent was evaporated under reduced pressure; the residue was triturated with acetone, dried, and recrystallized from (methanol: DMF) mixture (4:1).

***2-((5-(methyl((2-methyl-4-oxo-3,4-dihydroquinazolin-6-yl)methyl)amino)-1,3,4-thiadiazol-2-yl)thio)-N-phenylacetamide(S1).***

Yellow powder, yield 71%, m.p (215-217[0]C), Rf =0.23 (n-hexane: ethyl acetate: methanol 5:3:2). FTIR (υ, cm[−1]), 3479, 3375 (NH) str. of sec. amides, 3096 Ar (C-H) str., 1670 (C=O) str. of amide, 1612 (C=N) str.^{1}HNMR(DMSO-*d6*, 500MHz, δ=ppm): 2.51(s,3H,CH₃,quinazoline),2.89(s,3H, N-C$\underline{H}$₃), 4.22 (s, 2H, -C$\underline{H}$₂-S-), 4.89 (s,2H,C$\underline{H}$₂-N-), 7.06 (t,1H ,Ar-H) ,7.30 (m,2H, Ar-H), 7.56 (d,2H ,J=8.65, Ar-H),7.75 (d,1H, J= 8.36, Ar H), 8.02 (d,1H, J= 8.36, Ar-H) ,8.25 (s,1H, Ar-H), 10.48 (b s,1H,NH),12.86 (b s,1H,NH).^{13}CNMR (DMSO-*d6*, 125 MHz): 19.63, 31.79, 52.51, 58.37, 119.57, 119.96, 121.80, 124.03, 127.43, 129.26, 137.41, 138.74, 139.21,151.08,160.01,166.03,170.41.

***N-(4-chlorophenyl)-2-((5-(methyl ((2-methyl-4-oxo-3,4-dihydroquinazolin-6-yl) methyl) amino)-1,3,4-thiadiazol-2-yl)thio)acetamide (S2).***

Light brown powder, yield 66%, m.p (207-209[0]C), Rf =0.21(n-hexane: ethyl acetate: methanol 5:3:2). FTIR (υ, cm[−1]), 3479,3290 (NH) str. of sec amides ,3078 Ar(C-H), 1670 (C=O) str. of amide, 1612(C=N) str.^{1}HNMR(DMSO-d6, 500MHz, δ=ppm ): 2.38 (s,3H,CH₃,quinazoline)

,3.19 (s,3H,N-C$\underline{H}$₃) ,4.00 (s,2H,-C$\underline{H}$₂-S-),4.64(s,2H,C$\underline{H}$₂-N-),7.37(d,1H,J=8.55,Ar-H) ,7.61 (d,1H, J= 8.55, Ar-H), 7.67(d, 2H, J=8.47,Ar-H), 7.86 (d,2H,J=8.47, Ar-H) ,8.24 (s,1H,Ar-H). 10.46 (bs,1H,NH) ,12.41 (bs, 1H,NH) .^{13}C-NMR (DMSO-*d6*, 125 MHz) : 22.04, 31.51, 52.56, 59.42, 121.16, 121.22, 125.74, 127.78, 129.20, 130.95, 138.28, 149.26, 150.35, 156.43, 161.86, 166.44, 171.10.

***N-(4-methoxyphenyl)-2-((5-(methyl((2-methyl-4-oxo-3,4-dihydroquinazolin-6-yl)methyl)amino)-1,3,4-thiadiazol-2-yl)thio)acetamide (S3).***

Yellow powder, yield 68%, m.p (175-178[0]C), Rf =0.18 (n-hexane: ethyl acetate: methanol 5:3:2). FTIR (υ, cm[−1]), 3475,3379 (NH) str. of sec amides, 3037 Ar(C-H) ,1670 (C=O) str. of amide,1612 (C=N) str., 1226 (C-O) str. ^{1}HNMR(DMSO-*d6*,500MHz ,δ= ppm ): 2.38 (s,3H,CH₃, quinazoline), 3.21 (s,3H,N-C$\underline{H}$₃),3.71 (s,3H,O-C$\underline{H}$₃), 3.97(s,2H,-C$\underline{H}$₂-S-),4.66 (s,2H, C$\underline{H}$₂-N-), 6.88 (d,2H, J=8.50, Ar-H),7.49 (d, 2H, J=8.50, Ar-H),7.67(d,1H,J=8.38, Ar-H), 7.87(d,1H ,J=8.38, Ar-H), 8.24(s,1H, Ar-H) ,10.18 (b s ,1H ,NH) ,12.42 (b s,1H,NH). ^{13}CNMR (DMSO-*d6*, 125 MHz): 22.05, 31.48, 52.55, 55.63, 59.39, 114.35, 121.12, 12.19, 125.76, 127.75, 130.93, 132.39, 138.30, 149.48, 150.31, 155.83, 156.41, 161.84, 165.68, 171.03.

***2-((5-(methyl((2-methyl-4-oxo-3,4-dihydroquinazolin-6-yl)methyl)amino)-1,3,4-thiadiazol -2-yl)thio)-N-(4-nitrophenyl)acetamide (S4).***

Dark brown powder, yield 73%, m.p (161-163[0]C), Rf =0.17 (n-hexane: ethyl acetate: methanol 5:3:2). FTIR (υ, cm[−1]), 3471,3336 (NH) str. of sec amides, 3078 Ar (C-H) str. ,1670(C=O) str. of amide,1612 (C=N) str.,1496,1334 asymmetric and symmetric str. of (NO₂). ^{1}HNMR (DMSO-*d6*, 500MHz, δ=ppm): 2.38 (s,3H,CH₃, quinazoline),3.21 (s, 3H,N-C$\underline{H}$₃) ,4.09 (s,2H,-C$\underline{H}$₂-S-), 4.65 (s, 2H, C$\underline{H}$₂-N-),7.67(d,1H, J=8.35, Ar-H ),7.79(s,1H,Ar-H) , 7.85 (m, 3H, Ar-H), 8.23 (d,2H, J=8.56, Ar-H),10.95(bs,1H,NH),12.42(bs,1H,NH).^{13}CNMR (DMSO-*d6* ,125MHz): 22.04, 31.49, 52.55, 59.38, 119.32, 121.19 ,125.53, 125.75, 127.76, 130.93, 138.29,146.12,151.09,156.42,161.84,167.37, 171.03.

### In vitro cytotoxicity study
### Maintenance of cell cultures

Human breast cancer cell line (MCF-7), human lung cancer cell line (A549), and normal human fibroblast (NHF) cell line were grown in RPMI-1640 media supplemented with (FBS, 10%), penicillin (100IU/mL), and streptomycin (100 mg/mL). The cells were treated with the Trypsin-EDTA and re-seeded at 50% confluence twice a week then incubated at 37 °C [(22)].

### Cytotoxicity assay

To determine the cytotoxic effect, a cell viability assay was done using 96-well plates. Cell lines were seeded at $1 \times 10^4$ cells/well. When a confluent monolayer was achieved, cells were treated with the target compounds (S1-S4) separately at different concentrations (3.125, 6.25, 12.5, 25, 50, 100 µM) using methotrexate as a positive control. Cell viability was measured after 72h. of treatment by removing the medium, adding 28 µL of the MTT solution (2 mg/ml) and incubating the cells for 1.5 h. at 37 °C. After the removal of MTT solution, the remaining crystals were solubilized by the addition of 130 µL of DMSO and incubation for 15 min. at 37 °C with shaking [23]. The absorbency was measured at 492 nm using a microplate reader, the assay was performed in triplicate. The percentage of cytotoxicity (rate of cell growth inhibition) was calculated using the following equation [24,25]:

$$Cytotoxicity\ (\%) = A - B/\ A \times 100$$

Where A refers to the control optical density and B refers to the sample optical density.

### Molecular docking study

The chemical structures of the ligands were drawn by the ChemBioDraw program and then changed over into a 3D structure with the ChemBio3D computer program, energy minimization of the ligands was done by using the MM2 job and saved in the form of mol2 files, only the chain to which the co-crystallized ligand is bound was kept and all other chains were deleted. Water molecules, unnecessary ions, and other ligands were deleted also, hydrogen atoms were added and Gasteiger charges were assigned to simulate the *in vivo* conditions, the prepared protein was then saved as a (mol2) file. The co-crystallized ligands were selected and only the extracted ligands were used to define the binding sites. All protein atoms within 10 Å of each selected ligand were used for the binding site definition. The ligands were docked into the binding sites of the target enzymes using GOLD algorithm software [26]. The reliability of the docking process was validated using the x-ray structures of the co-crystallized ligands namely methotrexate for DHFR and raltitrexed for TS in the active sites of the target enzymes by redocking them into the corresponding binding sites, at the end of the docking run, the conformations of the ligands were ranked by their PLP-fitness scores, and the interactions were visualized in the Discovery Studio [27].

### In silico ADME prediction

SwissADME website makes it possible for researchers to compute physicochemical descriptors as well as pharmacokinetic parameters and drug-like properties of the designed molecules to support drug discovery [28]. Drug likeness and lipinski rule descriptors of the designed compounds are listed in (**Table 4**).

## Results and Discussion

### Chemistry

The synthesis of the intermediates and final compounds is shown in scheme 1. The purity of the products was confirmed by TLC in which a single spot for each compound was obtained. N-acylation of aniline or p-substituted anilines using chloroacetylchloride afforded compounds (A1-A4) in good yields, the reaction is carried out in presence of triethylamine, which acts as a base to neutralize HCl formed. The IR spectra of the synthesized compounds showed the disappearance of asymmetric and symmetric stretching vibration bands for $NH_2$ of the starting compounds (aniline and p-substituted anilines) and the appearance of new absorption band at 3263-3294 cm$^{-1}$ for NH stretching vibration of amide, the appearance of characteristic bands at 1662-1685 cm$^{-1}$ for C=O stretching vibration of amide (amide I band) and at 748-786 cm$^{-1}$ for C-Cl stretching vibration. Compounds A1-A4 were confirmed also via $^1$HNMR by the presence of a singlet peak for the amidic proton (CONH) at 10.11-10.82 ppm in addition to the singlet peak of ($CH_2$Cl) at 4.23-4.32 with an integration of 2 protons. Compound A3 was confirmed also by the presence of a characteristic singlet peak of 3 protons at 3.71 ppm due to ($OCH_3$). Characteristic peaks were also found at 165.04-169.32 ppm in the $^{13}$CNMR spectra attributed to the amide carbonyl group (CONH). Compounds (B1-B4) were prepared by S-Alkylation of 5-methylamino-1,3,4-thiadiazole-2-thiol with the chloroacetamide derivatives (A1-A4) in an alkaline aqueous medium (green reaction) in the presence of TEA to deprotonate the thiol group (SH) of 5-methylamino-1,3,4-thiadiazole-2-thiol and convert it to a thiolate anion (S$^-$) which acts as a strong nucleophile that attacks the carbon in the haloalkyl side chain of chloroacetamide intermediates to get the sulfide derivatives. The IR spectra of these compounds showed the disappearance of the absorption band of the SH group in the starting thiol compound at 2773 cm$^{-1}$, in addition to the presence of bands due to the secondary amine stretching vibration at 3282-3363cm$^{-1}$ and absorption bands at 1600-1616cm$^{-1}$ due to C=N stretching vibration of the thiadiazole ring. $^1$HNMR spectra of compounds (B1-B4) were characterized by the presence of a sharp singlet peak signified for 3 protons due to $CH_3$ of (NH$\underline{CH_3}$) at 2.83-2.88 ppm in addition to a broad singlet peak at 7.69-7.84 due to secondary amine proton ($\underline{NH}CH_3$). The final compounds (S1-S4) were prepared by N-alkylation of the secondary amine of 5-methylamino-1,3,4-thiadiazole-2-thiol with the alkyl bromide (6-(bromomethyl)-2-methyl-4(3H)-quinazolinone) in the presence of TEA to pick up the released HBr. The IR spectra of the final compounds showed the disappearance of the

absorption bands due to the secondary amine stretching vibration at 3282-3363cm⁻¹ and the appearance of new absorption bands in the range 3471-3479cm⁻¹ of NH stretching vibration of the quinazolinone amide group (CONH) which are shifted to higher frequency region. ¹HNMR spectra of the final compounds are characterized by the disappearance of the singlet peak at 7.69-7.84 due to secondary amine proton (NHCH₃), in addition to the appearance of all other signals which are

characteristics of the substituted 4(3H)-quinazolinone group that includes sharp singlet peak signified for 3 protons at 2.38 ppm due to the quinazolinone methyl group, sharp singlet at 4.64-4.66 ppm signified for 2 protons due to (CH₂-N-), multiplet peaks at 7.37-8.25 ppm attributed to the three protons of the fused benzene ring and broad singlet peak at 12.38-12.42 ppm due to quinazolinone amidic group (CONH).
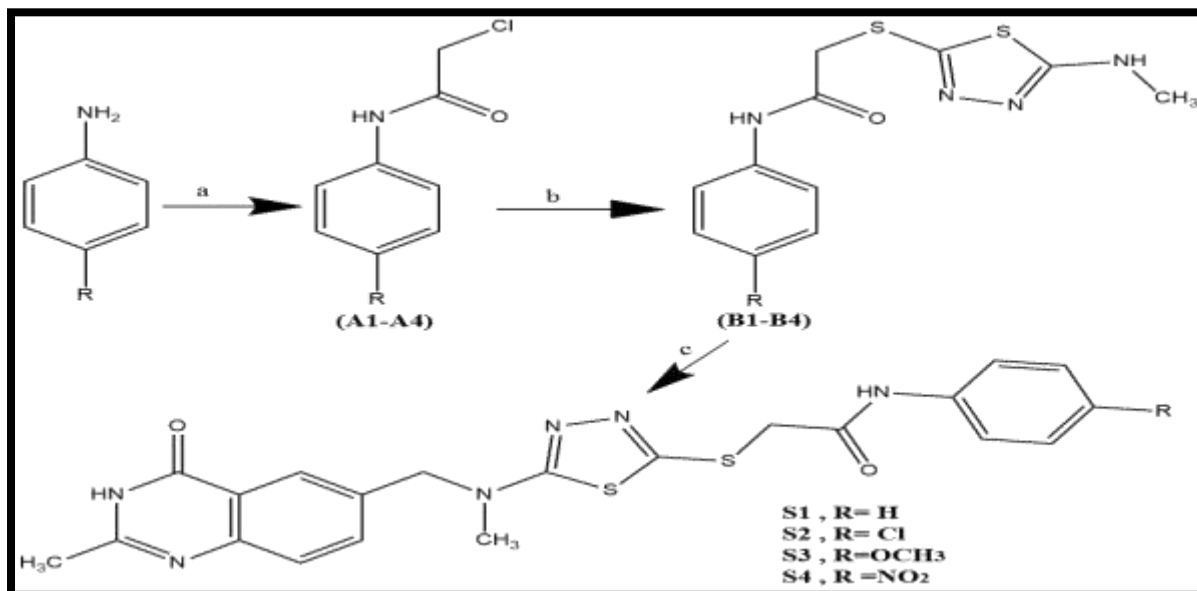


**Scheme 1**. Synthetic route of the target compounds (**S1-S4**). Reagents and condition: **a**. Chloroacetylchloride, TEA, dry benzene, reflux 3h. **b**. 5-methylamino-1,3,4-thiadiazole-2-thiol,distilled water ,TEA, room temperature 3h. **c**. 6-(bromomethyl) -2-methyl-4(3H)-quinazolinone, TEA, dry DMF, stirring overnight at 80⁰C.

### *In vitro cytotoxicity screening*

The synthesized compounds were evaluated for in vitro cytotoxic activity against various cell lines such as MCF-7 (breast cancer) and A549 (lung cancer) by the MTT assay method. To detect the selectivity of the tested compounds against cancer cells, epithelial cells derived from normal human fibroblast (NHF) were used also. The relationship between drug concentration and growth inhibition was plotted to obtain the survival curve of all cell lines MCF-7, A549, and NHF. Figure (**3**).The in vitro cytotoxic activities of the tested compounds are summarized in Table (**1**), whereas Figures (**4** and **5**) compare between the cytotoxicity of all compounds in relative to the positive control (MTX).The IC₅₀ values were used as a response parameter which refers to the concentration required to get 50% inhibition of cell viability [29] . All the compounds exhibited cytotoxic effects against the cancer cells higher than the normal cells, giving hope of the ability of these compounds to target cancer cells with a high degree of selectivity. The inhibition of growth exhibited by the tested compounds against the selected cell lines was parallel and in a concentration dependant manner.

Among the tested compounds, **S1** exhibited maximum cytotoxic activity against the MCF-7 cell line ( IC₅₀ 3.38 µM) and is about eight folds higher activity than methotrexate (IC₅₀ 27.32 µM).The cytotoxic activity against A549 cells showed that all the tested compounds displayed higher potency than methotrexate. The most potent one is compound **S2** (IC₅₀ 5.73µM) compared to methotrexate (IC₅₀ 259.4 µM). Apart from **S2**, compound **S1** was also found to be highly active (IC₅₀ 9.04 µM). The structure - activity relationships of the tested compounds related to MCF-7 revealed that compound **S1** (with no substituent at the para position of the anilide moiety) was the most potent one, compound **S3** (with the electron- donating methoxy group at the para position of the anilide moiety) was more potent (IC₅₀ 11.37 µM) than **S2** (IC₅₀ 57.1 µM) and **S4** (IC₅₀ 14.96 µM) with electron- withdrawing groups (Cl and NO₂) respectively. Conversely, the presence of electron-donating group at the para position of anilide moiety reduced the cytotoxicity against A549 cells , hence, compound **S3** was found to be less potent (IC₅₀ 29.12 µM) than both compounds **S2** and **S4** (IC₅₀ 5.73 and 16.75 µM) respectively .
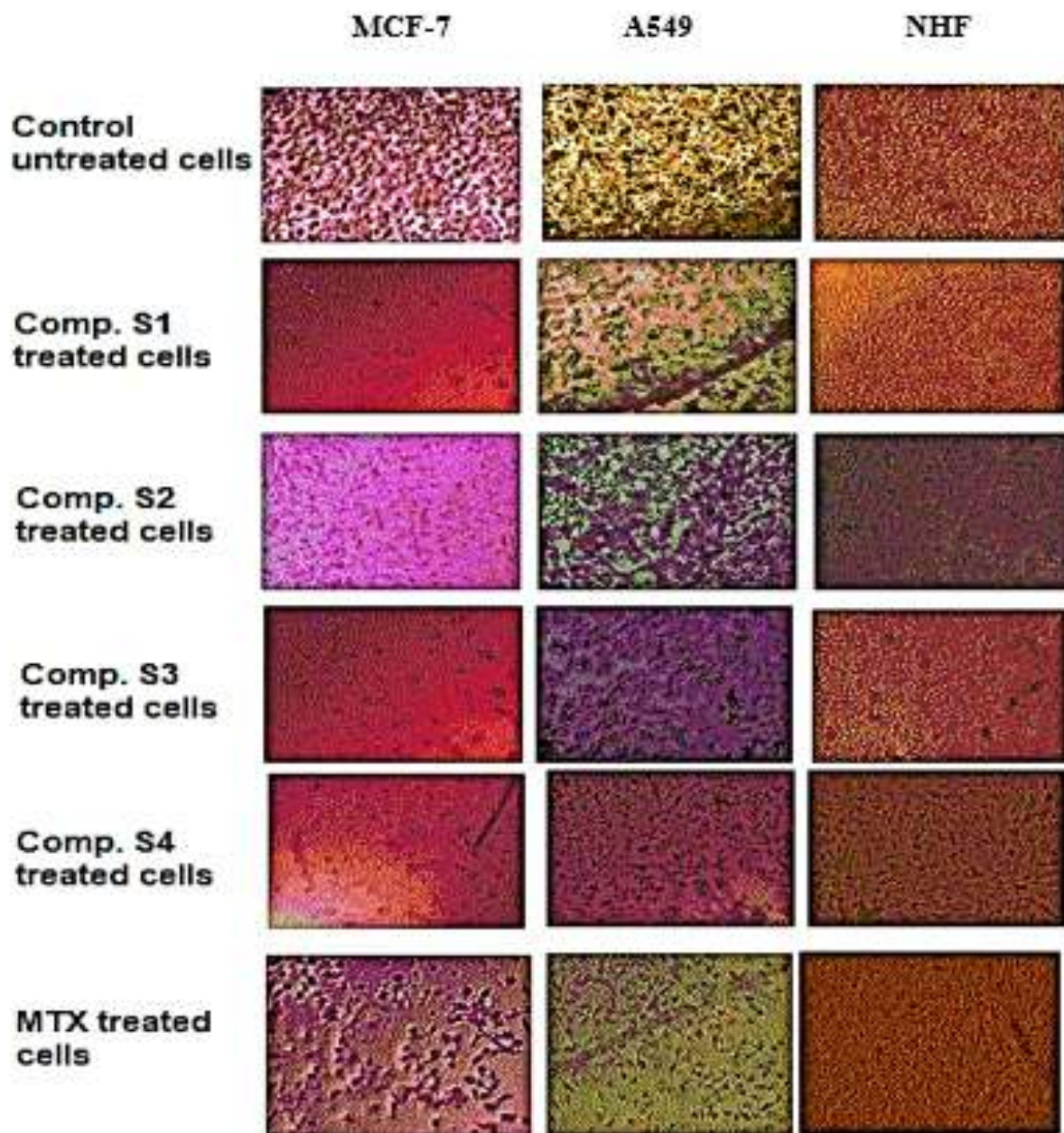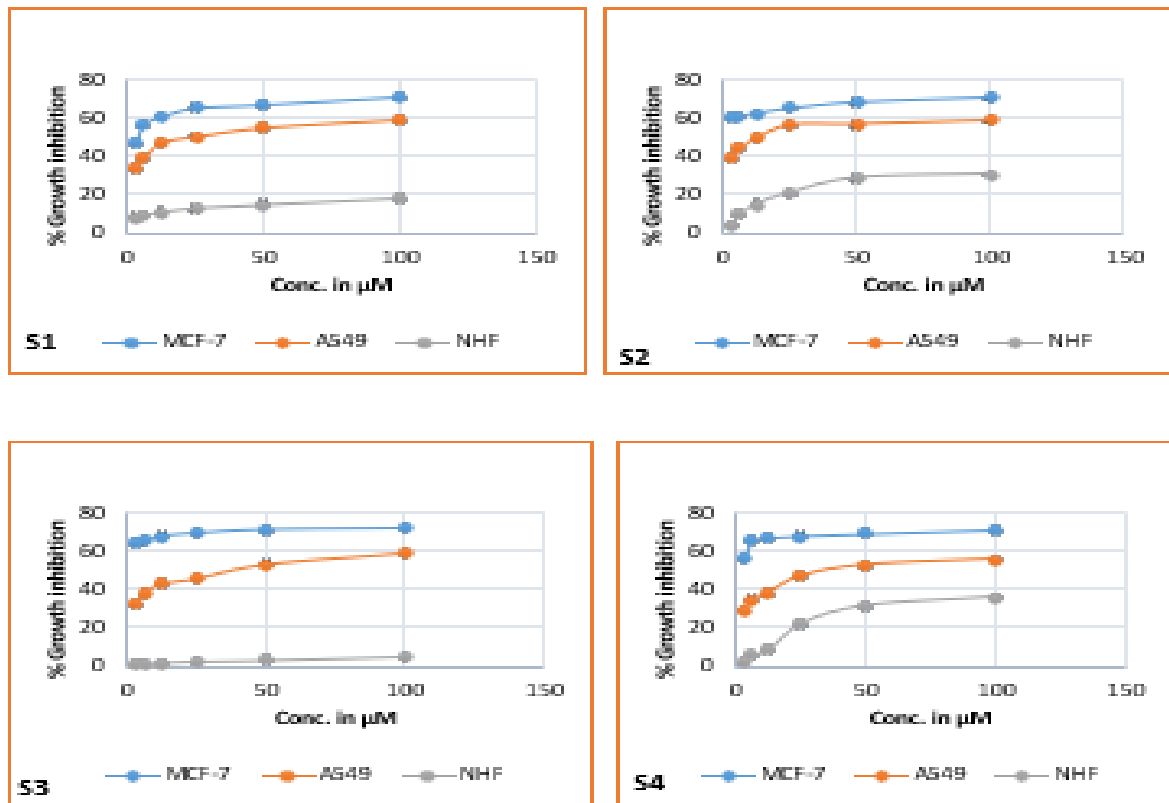
**Figure 2. Morphology of the cell lines after treatment with compounds (S1-S4) at their IC$_{50}$ concentrations. The cells were observed under an inverted microscope at 100× magnification.**

**Figure 3. Concentration vs. growth inhibition curve of compounds (S1-S4) against breast cancer cells (MCF-7) (blue), lung cancer cells (A549) (orange) and healthy fibroblast cells (NHF) (gray). (Values are represented by the mean ± SEM of triplicate measurements).**
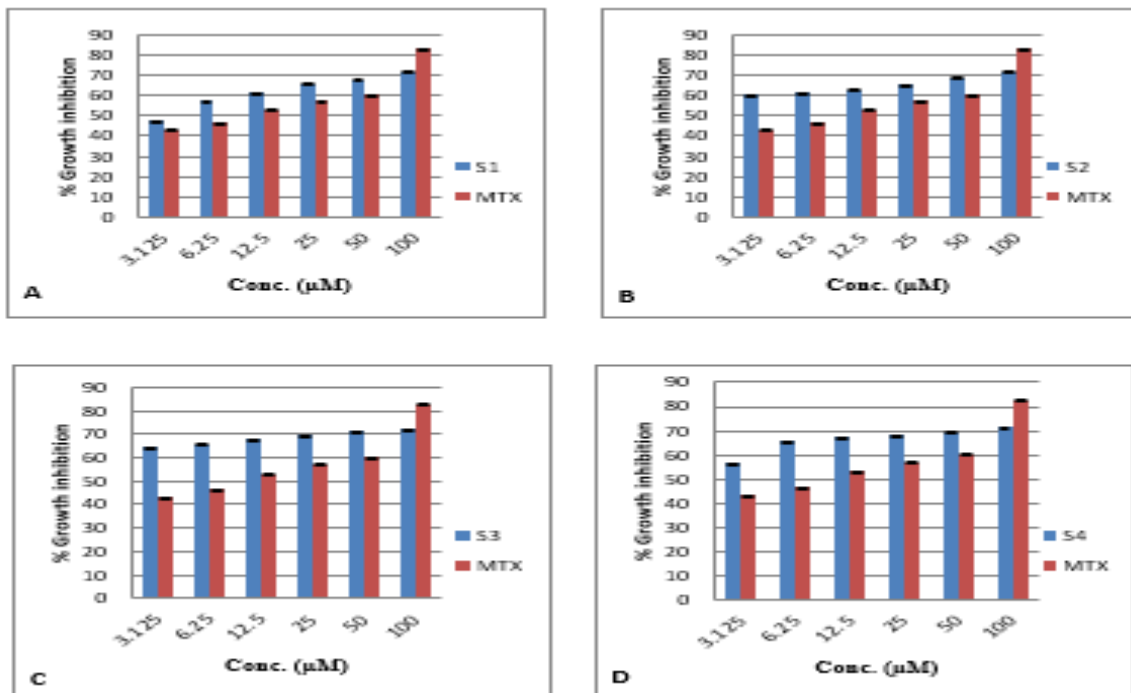


**Figure 4**. Histogram showing the concentration (µM) versus growth inhibition of the tested compounds: Compound S1 (**A**), Compound S2 (**B**), Compound S3 (**C**), and Compound S4 (**D**) against breast carcinoma cell line (MCF-7). (Values are represented by the mean ± SEM of triplicate measurements).
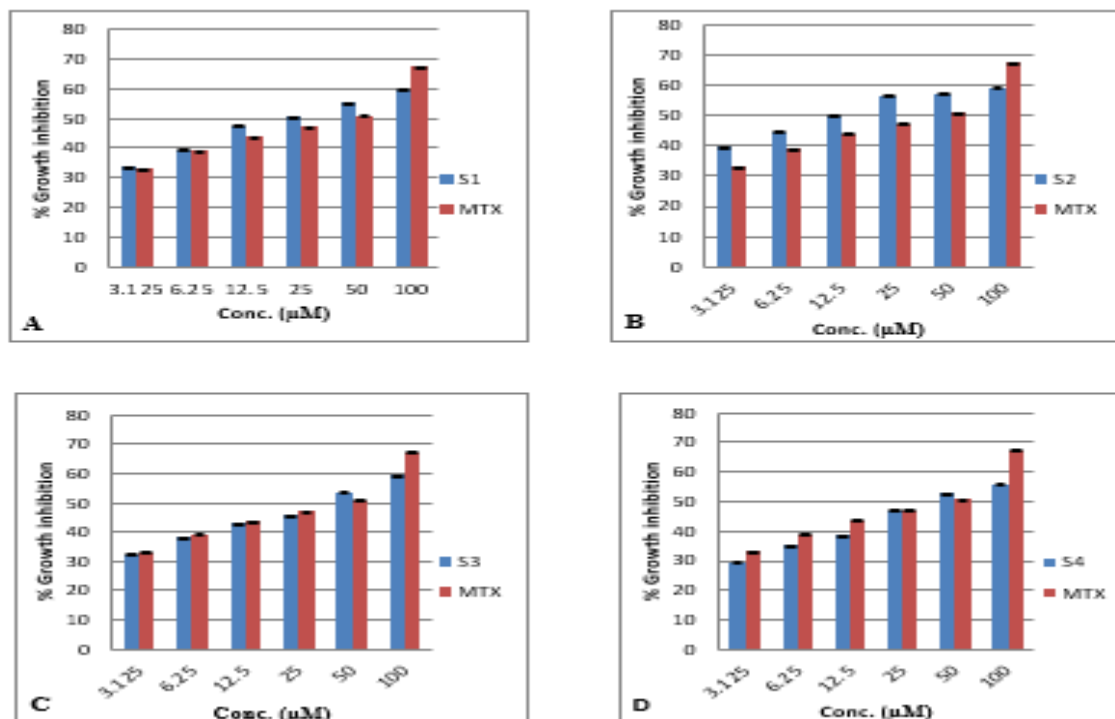
**Figure 5. Histogram showing the concentration (μM) and growth inhibition of the tested compounds: Compound S1 (A), Compound S2 (B), Compound S3 (C), and Compound S4 (D) against lung carcinoma cell line (A549). (Values are represented by the mean ± SEM of triplicate measurements).**

**Table 1. In-vitro cytotoxicity evaluation of the synthesized compounds against the selected cancer cells.**

| Compound | IC$_{50}$ (μM) | |
|---|---|---|
| | **MCF-7 cell line** | **A549 cell line** |
| S1 | **3.38** | 9.04 |
| S2 | 57.1 | **5.73** |
| S3 | 11.37 | 29.12 |
| S4 | 14.96 | 16.75 |
| MTX | 27.32 | 259.4 |

*Molecular docking study*

The docking study was carried out on compounds (S1-S4) as the ligands, where the complexes of DHFR and TS structures with their co-crystallized ligands (methotrexate and raltitrexed) respectively were selected as the docking models. For each docking, the parameters studied and compared were the PLP fitness score, number and length of hydrogen- bonds between ligand atoms and amino acid residues located in the binding site of the enzymes. All results are summarized in Tables (**2** and **3**). Captured images representing these ligand poses as well as hydrogen-bond interactions between the ligand and the enzymes are shown in Figures (**6** and **7**). Results of the docking study showed that all compounds exhibited good interactions with PLP fitness scores ranging from 93.21 to 95.93 against DHFR target protein and

from 71.33 to 81.97 against TS enzyme. The docking study against DHFR enzyme revealed that the most potent compound on the MCF-7 cell line (**S1**) exhibited a hydrogen-bonding interaction with the active site residue ARG 70 with a distance of 2.681Å through the carbonyl oxygen atom of the quinazolinone moiety and a hydrogen- bonding interaction between the carbonyl oxygen of the anilide and SER59 residue with 2.52 Å distance (Figure **6** (**B**)). The most potent compound against lung cancer cell line (**S2**) displayed different binding modes at the DHFR cavity in which it formed two hydrogen-bonding interactions between quinazolinone carbonyl oxygen atom and ARG31 residue with distances of 2.907 Å and 2.984 Å and two hydrogen- bonding interactions between the two thiadiazole nitrogen atoms and ARG31 residue with distances of 2.86 Å and 3.021 Å in addition to one hydrogen bonding interactions between the anilide NH group and GLU35 residue with a bond length of 2.942 Å (Figure **6** (**C**)). Docking study of methotrexate on the DHFR enzyme showed that the polar glutamate tail was involved in the formation of four hydrogen bonds with ARG31 and ARG70 residues (Figure **6** (**A**)). From the above results, it could be concluded that both compounds **S1** and **S2** displayed partially the same binding pattern of methotrexate with DHFR target protein. This confirms that binding interactions with both ARG31 and ARG70 residues were essential for DHFR inhibition and improving the cytotoxic activity against the two cancer cell lines**.** Docking study on TS enzyme revealed that compound **S1** formed only

one hydrogen-bonding interaction with the active site residue LEU221 with a distance of 2.909 Å through the NH group of the anilide moiety (Figure **7** (**B**)), while compound **S2** formed a hydrogen-bonding interaction between the carbonyl oxygen of the anilide and ASN112 residue at 3.067 Å distance (Figure **7** (**C**)). In comparison with raltitrexed, it was shown that the most potent compound against lung carcinoma cells (**S2**) displays in part a similar binding pattern with raltitrexed since both of them showed hydrogen bonding interactions with ASN112 (Figure **7** (**A**)).

**Table 2. Docking study data showing amino acid interactions and the hydrogren bond lengths of target compounds and methotrexate on DHFR (PDB: 3EIG).**

| Compound no. | Chem PLP score | no. of H-bonds | Atoms of compound forming H-bond | Amino acid residues forming H-bonds (H-bond length in Å) |
|---|---|---|---|---|
| S1 | 93.21 | 2 | Quinazolinone C=O (H-bond acceptor). Anilide C=O (H-bond acceptor). | ARG70 (2.681) SER59 (2.520) |
| S2 | 94.97 | 5 | Quinazolinone C=O (2 bonds) (H-bond acceptors). Thiadiazole N (2 bonds) (H-bond acceptors). Anilide NH (H-bond donor). | ARG31 (2.907) ARG31 (2.984) ARG31 (2.860) ARG31 (3.021) GLU35 (2.942) |
| S3 | 93.88 | 1 | Quinazolinone C=O (H-bond acceptor) | ARG31 (2.630) |
| S4 | 95.93 | 2 | Anilide C=O (H-acceptor). Anilide NH (H-bond donor). | ARG31(2.864) GLU35 (2.954) |
| Methotrexate | 99.41 | 9 | Pteridine NH$_2$ (2 bonds) (H-bond donors). Pteridine NH$_2$ (H-bond donor). N-CH$_3$ (H-bond acceptor). Amide C=O (H-bond acceptor). Glutamate α COOH (2 bonds) (H-bond donor and acceptor). Glutamate γ COOH (2bonds) (H-bond donor and acceptor). | Val115(2.712) ILE7(2.640) GLU30(2.753) SER59(2.580) ASN64(2.685) ARG70(2.957, ARG70(2.964) ARG31(2.886) ARG31(3.027) |

**Table 3. Docking study data showing amino acid interactions and the hydrogen bond lengths of target compounds and methotrexate on TS (PDB: 5X5Q).**

| Compound no. | Chem PLP score | No. of H-bonds | Atoms of compound forming H-bond | Amino acid residues forming H-bonds (H-bond length in A° ) |
|---|---|---|---|---|
| S1 | 71.33 | 1 | Anilide NH(H-bond donor) | LEU221(2.909) |
| S2 | 74.28 | 1 | Anilide C=O (H-bond acceptor) | ASN112(3.067) |
| S3 | 78.28 | 2 | OCH₃(2 bonds) (H-bond acceptor) | ARG78(2.997) ARG78(2.989) |
| S4 | 81.97 | 4 | Quinazolinone NH(H-bond donor) Anilide C=O (H-bond acceptor) NO₂ (2 bonds) (H-bond acceptors). | ARG78(3.068) ASP218(3.057) ARG50(3.022) TYR258(2.778) |
| Raltitrexed | 78.43 | 5 | Glutamate α COOH (2 bonds) (H-bond donor and acceptor). Glutamate γ COOH (3 bonds) (1H-bond donor and 2H-bond acceptors). | ARG50(2.818) ASN112(2.913) ARG215(2.894) ARG215(3.04) ARG50(2.867) |
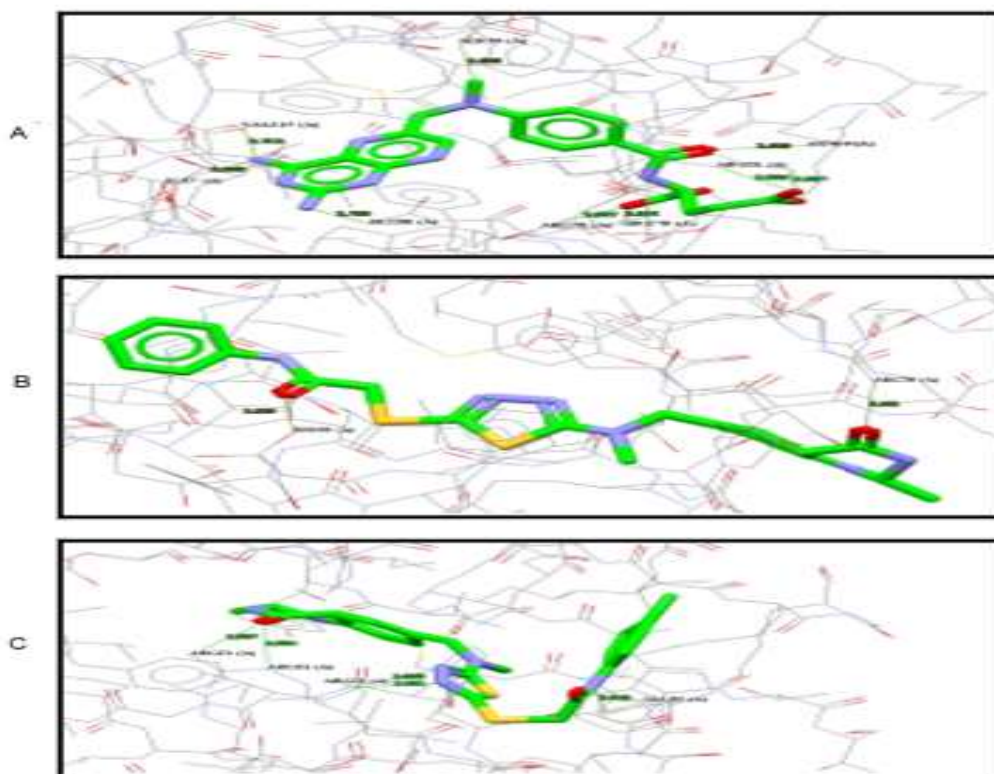


 **Figure 6**. Comparison of binding mode of methotrexate (**A**), compound S1 (**B**), and compound S2 (**C**) into the binding site of DHFR (PDB: 3EIG). The key amino acid residues are represented by black sticks. Hydrogen bonds are shown as green dashes.
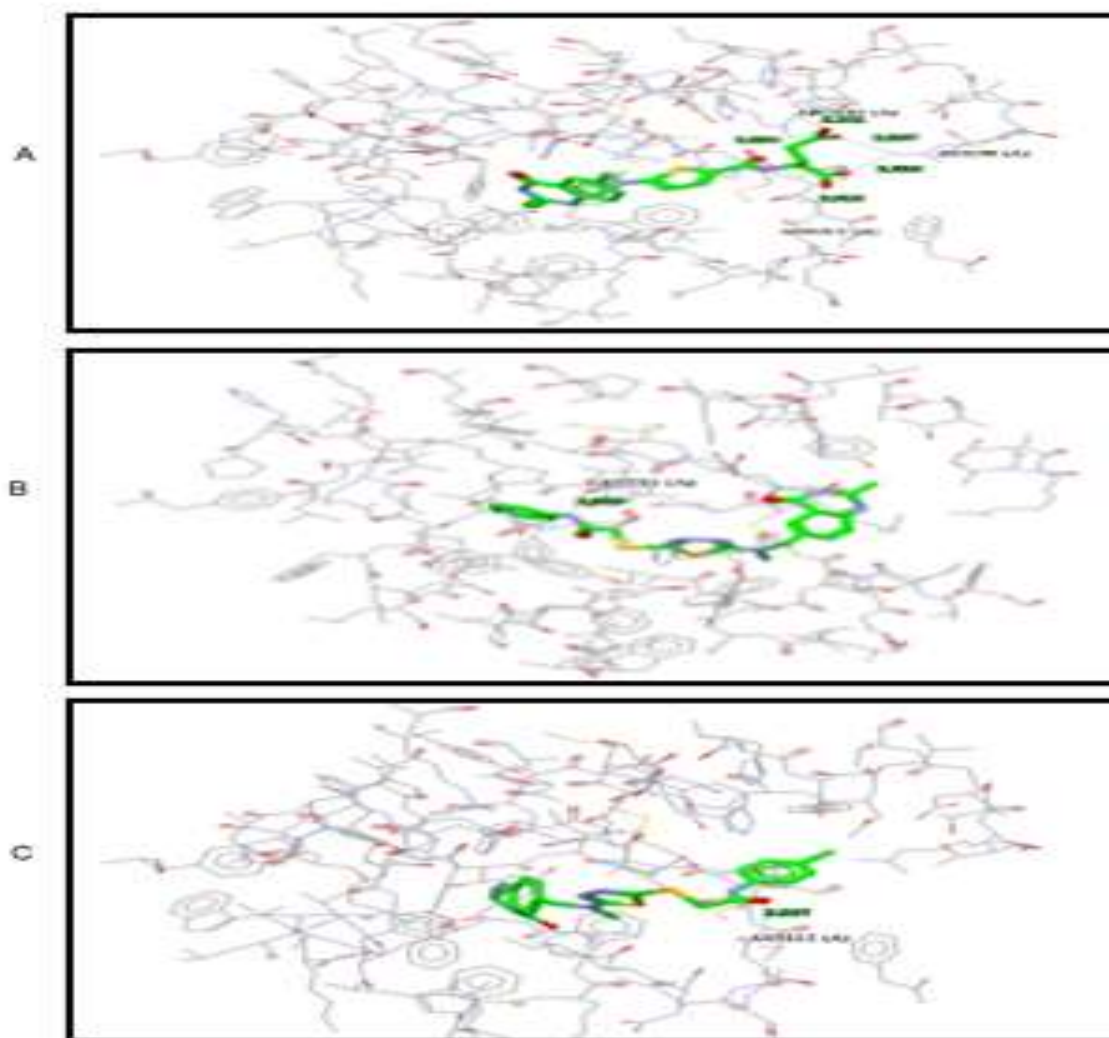
**Figure 7. Comparison of binding mode of raltitrexed (A), compound S1 (B), and compound S2 (C) into the binding site of TS (PDB: 5X5Q). The key amino acid residues are represented by black sticks. Hydrogen bonds are shown as green dashes.**

### *In silico ADME Prediction*

The physicochemical properties of drugs play an important role in their biological effects, one of the most critical parameters is the partition coefficient (Clog $P_{o/w}$) which gives an expectation about the way of drug transport within the body [30].

Clog $P_{o/w}$ values of all the synthesized compounds were less than five. The compounds also displayed an acceptable bioavailability scores (0.55). With the exception of compound S3, the designed compounds were also seemed not to be substrates for the multidrug resistance protein (P-glycoprotein).

**Table 4**. Drug likeness and lipinski rule descriptors of the target compounds.

| Comp. | M.Wt | No. of H-bond acceptors | No. of H-bond donors | TPSA* | C Log $P_{o/w}$ | Lipinski violation | Pgp substrate | Bioavailability Score |
|---|---|---|---|---|---|---|---|---|
| S1 | 452.55 | 5 | 2 | 157.41 | 2.93 | 0 | NO | 0.55 |
| S2 | 486.99 | 5 | 2 | 157.41 | 3.54 | 0 | NO | 0.55 |
| S3 | 482.58 | 6 | 2 | 166.64 | 2.98 | 0 | YES | 0.55 |
| S4 | 497.55 | 7 | 2 | 203.23 | 2.23 | 1 | NO | 0.55 |

*TPSA: Total Polar Surface Area

## Conclusion

New derivatives of 4(3H)-quinazolinones bearing 1,3,4-thiadiazole moiety were synthesized and evaluated against (MCF-7) and (A549) human cancer cell lines. Compounds S1 and S2 could be good candidates as anticancer agents. However, many pharmacological and toxicological studies are still required to confirm the therapeutic benefits of the new derivatives.

## Acknowledgments

## References

1. Mahsa Toolabi , Setareh Moghimi , Tayebeh Oghabi Bakhshaiesh , Somayeh Salarinejad , Ayoub Aghcheli , Zaman Hasanvand , Elahe Nazeri , Ali Khalaj ,Rezvan Esmaeili ,Alireza Foroumadi ,6-Cinnamoyl-4-arylamino thieno-pyrimidines as highly potent cytotoxic agents: Design, synthesis and structure-activity relationship studies. Eur. J. Med. Chem. 2020; (185):111786.
2. Mohamed A Abdelsalam, Omaima M AboulWafa, El-Sayed AM Badawey, Mai S El-Shoukrofy, Mostafa M El-Miligy & Noha Gouda. Design and synthesis of some β-carboline derivatives as multi-target anticancer agents. Future Med. Chem. 2018; 10(24): 2791–2814.
3. Dennis L. Wright and Amy C. Anderson, Antifolate Agents: A Patent Review (2006–2010), Expert Opin. Ther. Pat. 2011; 21(9): 1293–1308.
4. Chan DCM, Anderson AC. Towards species-specific antifolates. Curr Med. Chem. 2006; 13(4):377–398.
5. Filiz Esra Önen Bayram, Hande Sipahi and Hülya Akgün, Acetylenic antifolates as anticancer agents. Pteridines 2015; 26(3): 85–92.
6. Du-Jong Baek, Tae-Beom Kang, and Hyun Ju Kim; Synthesis of Nonclassical Quinazolinone Antifolates as Thymidylate Synthase Inhibitors and Their Antitumor Activity In Vitro. Bull. Korean Chem. Soc. 2004; 25 (12):1898-1906.
7. Aleem Gangjee, Yibin Qiu, Wei Li, and Roy L. Kisliuk, Potent Dual Thymidylate Synthase and Dihydrofolate Reductase Inhibitors: Classical and Nonclassical 2-Amino-4-oxo-5-arylthiosubstituted-6-methylthieno[2,3-d] pyrimidine antifolate . J. Med. Chem. 2008 ; 51(18): 5789–5797.
8. Gangjee A, Kurup S, Namjoshi O. Dihydrofolate Reductase as a Target for Chemotherapy in Parasites. Curr. Pharm. Des. 2007; 13(6):609–639.
9. Ola A. Abdelaziz, Walaa M. El Husseiny, Khalid B. Selim, Hassan M. Eisa. Dihydrofolate reductase inhibition effect of 5-substituted pyrido [2,3-d] pyrimidines: Synthesis, antitumor activity and molecular modeling study. Bioorg. Chem. 2019; 90: 103076.
10. Farshid Hassanzadeh , Hojjat Sadeghi-aliabadi , Shadan Nikooei , Elham Jafari, and Golnaz Vaseghi, Synthesis and cytotoxic evaluation of some derivatives of triazole quinazolinone hybrids. Res. Pharm. Sci. 2019; 14(2): 130-137.
11. Jafari E, Rahmani Khajouei M, Hassanzadeh F, Hakimelahi GH, Khodarahmi GA. Quinazolinone and quinazoline derivatives: recent structures with potent antimicrobial and cytotoxic activities. Res. Pharm. Sci. 2016; 11(1):1-14.
12. Vaseghi G, Jafari E, Hassanzadeh F, HaghjooyJavanmard S, Dana N, Rafi eian-Kopaei M. Cytotoxic evaluation of some fused pyridazino- and pyrrolo-quinazolinones derivatives on melanoma and prostate cell lines. Adv. Biomed. Res. 2017; 6:76.
13. Elham Taherian, Ghadamali Khodarahmi, Marzieh Rahmani Khajouei, Farshid Hassanzadeh , and Nasim Dana, Synthesis and cytotoxic evaluation of novel quinozalinone derivatives with substituted benzimidazole in position 3, Res. Pharm. Sci. 2019; 14(3): 247-254.
14. Mehlika Dilek Altıntop , ID , Halil Ibrahim Ciftci , Mohamed O. Radwan , Belgin Sever ,Zafer Asım Kaplancıklı , Taha F. S. Ali , Ryoko Koga , Mikako Fujita , Masami Otsuka , and Ahmet Özdemir. Design, Synthesis, and Biological Evaluation of Novel 1,3,4-Thiadiazole Derivatives as Potential Antitumor Agents against Chronic Myelogenous Leukemia: Striking Effect of Nitrothiazole Moiety. Molecules 2018; 23(1): 59.
15. Volpato JP, Yachnin BJ, Blanchet J, Guerrero V, Poulin L, Fossati E, Berghuis AM, Pelletier JN, Multiple conformers in active site of human dihydrofolate reductase F31R/Q35E double mutant suggest structural basis for methotrexate resistance. J. Biol. Chem. 2009; 284: 20079-20089.
16. Chen, D., Jansson, A., Sim, D., Larsson, A., Nordlund, P. Structural analyses of human thymidylate synthase reveal a site that may control conformational switching between active and inactive states. J. Biol. Chem. 2017; 292: 13449-13458.
17. Berman, H. M.; Westbrook, J.; Feng, Z.; Gilliland, G.; Bhat, T. N.; Weissig, H.; Shindyalov, I. N.; Bourne, P. E. The Protein Data Bank. Nucleic Acids Res. 2000; 28: 235–242.
18. Muthanna Saadi Farhan and Kawkab Y. Saour. Synthesis of Some Heterocyclic Compounds

Linked to Amino Acid Esters with Expected Biological Activities. Ph.D Research Thesis, Department of pharmaceutical chemistry, University of Baghdad, college of pharmacy. Iraq; 2013.pp.58.

19. N. Azizi, A. Khajeh Amiri, M. Bolourtchian and M.R. Saidi, A Green and Highly Efficient Alkylation of Thiols in Water, J. Iran. Chem. Soc. 2009; 6(4): 749-753.

20. Mohammed Hassan Mohammed, Monther Faisal Mahdi, Noor Hatef Naser Sulaf Majeed Ali, Design, Synthesis and Pharmacological Evaluation of Sulfanilamide-Ciprofloxacin Conjugates Utilizing Hybridization Approach as New Antibacterial Agents, J. Nat. Sci. Res. 2015; 5(4).106-117.

21. Asadi P, Khodarahmi GhA, Jahanian-Najafabadi A, Saghaie LA, Hassanzadeh F. Synthesis, characterization, molecular docking studies and biological evaluation of some novel hybrids based on quinazolinone, benzofuran and imidazolium moieties as potential cytotoxic and antimicrobial agents. Iran J. Basic Med. Sci. 2017; 20:975-989.

22. Al-Shammari AM, Alshami MA, Umran MA, Almukhtar AA, Yaseen NY, Raad K, et al. Establishment and characterization of a receptor-negative, hormone-nonresponsive breast cancer cell line from an Iraqi patient. Breast Cancer: Targets Ther. 2015; 7:223-230.

23. Abdullah SA, Al-Shammari AM, Lateef SA. Attenuated measles vaccine strain have potent oncolytic activity against Iraqi patient derived breast cancer cell line. Saudi J. Biol. Sci. 2020; 27(3):865-872.

24. Khashan, K. S., Jabir, M. S., & Abdulameer, F. A. Carbon Nanoparticles prepared by laser ablation in liquid environment. Surface Review and Letters 2019; 26(10): 1950078.

25. Kareem, S. H., Naji, A. M., Taqi, Z. J., & Jabir, M. S. PolyvinylpyrrolidoneLoaded-MnZnFe2O4 Magnetic Nanocomposites Induce Apoptosis in Cancer Cells Through Mitochondrial Damage and P 53 Pathway. J Inorg. & Organmet. Poly. & Mat. 2020; 1-15.

26. Marcel L. Verdonk, Jason C. Cole, Michael J. Hartshorn, Christopher W. Murray, and Richard D. Taylor. Improved Protein–Ligand Docking Using GOLD. PROTEINS: Structure, Function, and Genetics 2003; 52:609 – 623.

27. N. Fayyazi, A. Fassihi, S. Esmaeili et al., Molecular dynamics simulation and 3D-pharmacophore analysis of new quinoline-based analogues with dual potential against EGFR and VEGFR-2, Int. J. Biol. Macro. 2020; 142:94-113.

28. Antoine Daina, Olivier Michielin, and Vincent Zoete. SwissADME: a free web tool to evaluate pharmacokinetics, drug-likeness and medicinal chemistry friendliness of small molecules. Scientific Reports 2017; 7: 42717.

29. Srikanth Gatadi, Gauthami Pulivendala, Jitendra Gour, Satyaveni Malasala, Sushmitha Bujji, Ramulu Parupalli, Mujahid Shaikh, Chandraiah Godugu, Srinivas Nanduri. Synthesis and evaluation of new 4(3H)-Quinazolinone derivatives as potential anticancer agents. J. Mol. Str. 2020; 1200:127097.

30. Abbas AH, Razzak Mahmood AA, Tahtamouni LH, Al-Mazaydeh ZA, Rammaha MS, Alsoubani F, Al-bayati RI . A novel derivative of picolinic acid induces endoplasmic reticulum stress-mediated apoptosis in human non-small cell lung cancer cells: synthesis, docking study, and anticancer activity. Pharmacia 2021; 68(3): 679–692.